

Total Solar Irradiance Variability: A Review

Judit M. Pap

*1 Division of Astronomy and Astrophysics, University of California, 1 Los Angeles
8979 MSA, 405 Hilgard Ave., Los Angeles, CA 90095-1562

In "*Past and Present Variability of the Solar-Terrestrial System:
Measurement, Data Analysis and Theoretical Models*", Enrico Fermi
Summer School, Varenna, Italy, June 25 - July 5, 1996.

* On leave of absence from the Jet Propulsion Laboratory, California Institute of Technology,
MS 169-506, 4800 Oak Grove lb., Pasadena, CA 91109

Abstract

Observations of total solar irradiance from space within the last two decades convinced the skeptics that total irradiance varies over a wide range of periodicities: from minutes to the 11-year solar activity cycle. Analyses based on these space-borne observations have demonstrated that the irradiance variations are directly related to changes at the photosphere and the solar interior. It has been shown that the long-term irradiance changes over the solar cycle represent real luminosity changes. Theoretical considerations and modeling efforts indicate that irradiance models based on the surface manifestations of solar magnetic activity are not sufficient to explain all the aspects of the observed irradiance variations. Global effects, such as changes in the solar diameter, surface temperature, the differential rotation in the Sun's interior, solar dynamo magnetic fields near the bottom of the convective zone, and large-scale convective cells may also produce variations in total irradiance. These results underscore the importance of space irradiance monitoring programs and demonstrate that high precision and accurate irradiance observations are inevitable to study the climate response to solar variability.

1 Introduction

The accurate knowledge of the solar radiation received by the Earth and its temporal variations is critical for an understanding of the role of solar variability in climate changes and the climate response to increasing greenhouse gas concentrations. The value of the integrated solar energy flux over the entire spectrum, hence total irradiance, arriving at the top of the terrestrial atmosphere at the mean Sun-Earth distance is called "solar constant". The concept of the solar constant was introduced in the last century. The first measurements of the direct solar radiation were performed by Pouillet in 1837. Continuous observational programs of total solar irradiance to detect its variability started as early as the beginning of this century at the Smithsonian Institute; first from high altitude mountain stations, later on from balloons and aircraft. The first attempts to measure total irradiance outside of the terrestrial atmosphere were made in

the sixties from rockets and the Mariner space probes. [10WCVC], these early measurements were inconclusive and could not reveal real solar changes in total irradiance because of the lack of sufficient radiometric precision and the selective absorption of the terrestrial atmosphere [1].

Considerable improvement in radiometry took place in the sixties, when a new generation of radiometers, the so-called electrically self-calibrating active cavity radiometers, were developed in various U.S. and European institutions [2,3,4,5]. These new radiometers are capable of measuring total solar irradiance with an absolute accuracy of $\pm 0.2\%$, the precision of the measurements, however, is much higher. In addition to the significant improvement in radiometry, long-term flight opportunities from various satellite platforms have made it possible to monitor total solar irradiance above the Earth's atmosphere since the late seventies.

Irradiance observations performed from space within the last two decades established conclusively that the value of the solar constant is not constant and the variations in total solar irradiance from days to years are directly related to changes at the photosphere and in the solar interior [6,7,8]. Although the existence of possible global changes basal on the changing solar output had been doubted and debated for a long time, the results of various space experiments for monitoring total irradiance opened an exciting new era in both atmospheric and solar physics. One of the main interests is to reconstruct solar irradiance changes back to the time of the Maunder Minimum (1645-1705), when the unexceptionally low magnetic activity of the Sun was accompanied with a cold period in Europe and the Atlantic region, known as Little Ice Ages [9,10]. In addition to the climate implication of total irradiance variations, the observation and interpretation of total irradiance variability have also led to new ways of understanding of the structure and the dynamics of the Sun on a global scale. The ultimate goal is to uncover how and why the Sun is changing on human times scales in order to reconstruct and predict the solar-induced climate changes.

2 Variations Observed in Total Solar Irradiance

The time series of various space observations of total solar irradiance are plotted in Fig. 1, which has been provided by the SOHO/VIRGO Science Team for this paper [11]. The different scale of these measurements is related to the absolute accuracy ($\pm 0.2\%$) of the calibration of the individual instruments [7]. Because of the low absolute accuracy of the current total irradiance measurements, it is extremely difficult to maintain long-term homogenous irradiance datasets, especially when there are interruptions in the observed data.

The first and longest high precision space total irradiance monitoring program was carried out by radiometer III^F of the "Earth Radiation Budget" (ERB) experiment on the Nimbus-7 satellite between November 1978 and January 1993 [12]. The "Active Cavity Radiometer Irradiance Monitoring 1" (ACRIM 1) experiment on the Solar Maximum Mission (SMM) satellite was launched on February 14, 1980 and was operated by the end of November 1989 [13]. The ACRIM 1 experiment was followed by the ACRIM II on board the Upper Atmosphere Research Satellite (UARS), which was launched in September 1991 [14] and it is still operating as of this time. Instruments almost identical to ACRIM have been flown by NASA's "Earth Radiation Budget Experiment" (ERBE) on board the Earth Radiation Budget Satellite (ERBS) since October 1984 and on the NOAA-9 and NOAA-10 satellites since January 1985 and October 1986, respectively [15]. The UARS/ACRIM II irradiance values plotted in Fig. 1 have been adjusted to the ACRIM 1 level via the intercomparison of the two sets of ACRIM data with the ERB-III^F and ERBS irradiance measurements [16].

The "Solar Variability" (SOVA) experiment on board the European Retrievable Carrier (EURICA) was launched on July 31, 1992 and it was retrieved in June 1993. The SOVA experiment consisted of two types of absolute radiometers: the "Differential Dual Absolute Radiometer" (DARAD) of the SOVA1 experiment [17] and the PMO-6 type of absolute radiometer of the SOVA2 experiment [18]. In addition to the radiometers, both SOVA1 and SOVA2 experiments included sunphotometers which measured solar spectral irradiance between 335

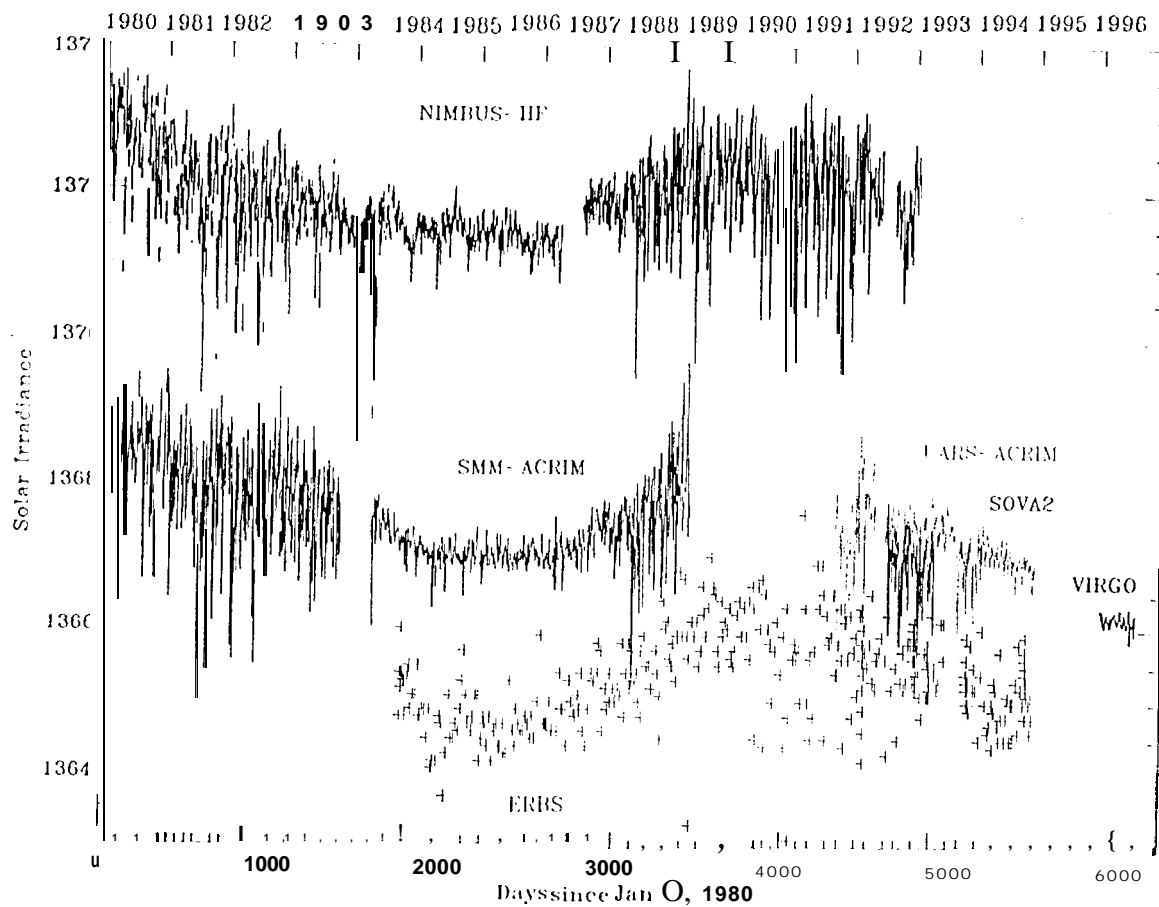


Fig. 1.: Time series of various space-borne irradiance experiments are presented from the late seventies to up-to-date. Note that Fig. 1 was provided for this paper by the courtesy of the SOHO/VIRGO Science Team[1 1].

and 862 nm. More recently, total solar irradiance has been monitored by the “Variability of Irradiance Gravity Oscillations” (VIRGO) experiment on board the Solar Heliospheric Observatory (SOHO). The VIRGO experiment carries two radiometers (1)1 A RAD and 1 PMO6-V), sunphotometers measuring spectral irradiance at 402, 500, and 862 nm, and a low resolution “Luminosity oscillation Imager” (1,01) [19]. The SOHO/VIRGO observations provide unique irradiance datasets since SOHO is placed at the Sun-Earth Lagrange 1 (L1) point, where continuous observations of the Sun are possible.

Although the absolute accuracy of the total irradiance measurements is limited to about $\pm 0.2\%$, the precision and stability of the instruments is much better, which makes it possible to study the relative variations in total irradiance. As illustrated in Fig. 1, total solar irradiance varies over a wide range of periodicities. The most important discovery of the satellite-based irradiance observations is that total solar irradiance varies by about a small fraction of 1 % over the solar cycle, being higher during maximum solar activity conditions [6,7]. This solar-cycle-related variation of total solar irradiance is attributed to the changing emission of bright magnetic elements. It has been demonstrated that the active regions faculae alone fails by more than a factor of two in explaining the solar-cycle-related long-term changes [20]. A third component, the so-called “active network” has been introduced to explain the observed long-term irradiance changes [21]. It has been shown that the long-term irradiance changes may also be related to variations in the photospheric temperature [20], however, it is not yet clear whether this change can be linked with the bright network component.

The short-term changes on time scales of days to months are associated with the evolution of active regions via the combined effect of dark sunspots and bright faculae [22]. The most striking events in the short-term irradiance changes are the sunspot-related dips in total irradiance with an amplitude up to 0.3%, whereas faculae can enhance the total flux with an amplitude of about 0.08% [23]. A particular dip in total irradiance, observed in late June and early July of 1988 is presented in Fig. 2. The solid line on the lower panel shows the ACRIM 1 total irradiance. The corresponding solar images, taken at the San Fernando Observatory, California

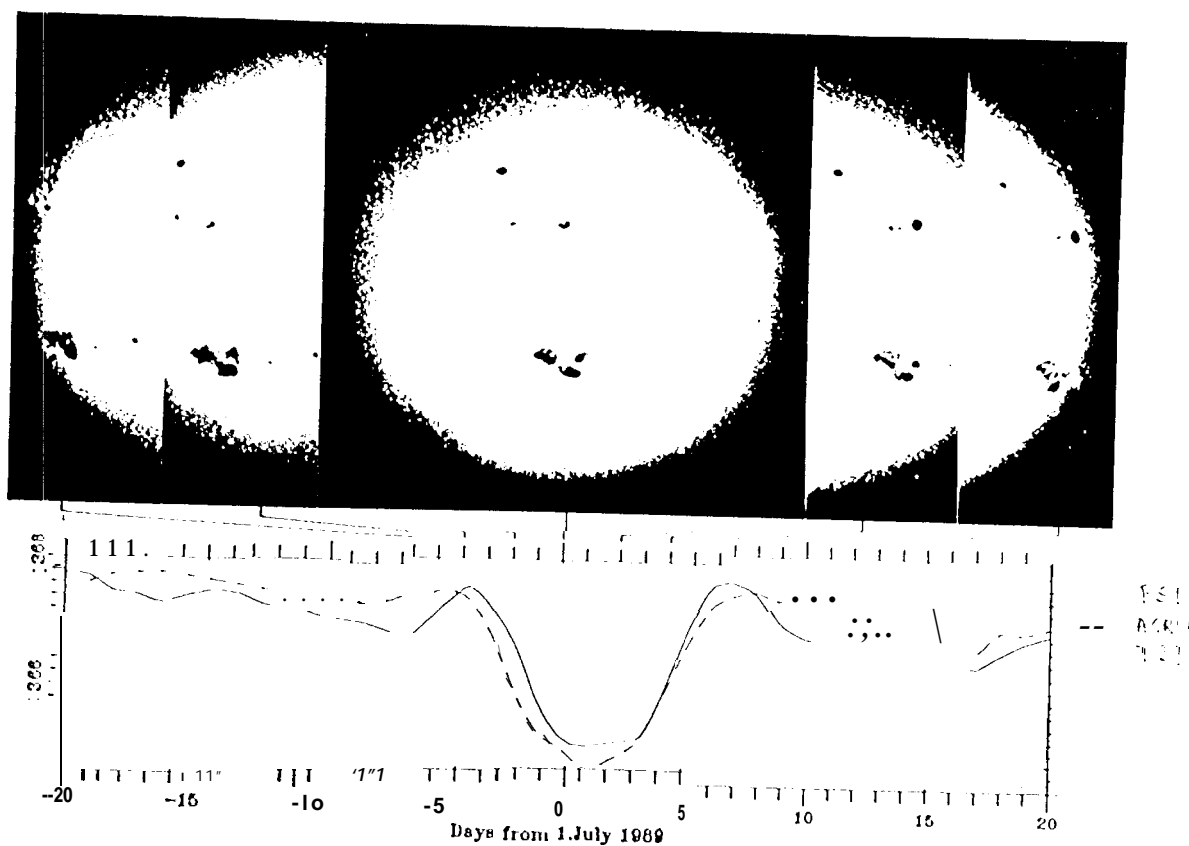


Fig. 2.: An individual dip in total irradiance caused by a large sunspot group in late June and early July, 1988 is presented on the lower panel. The solid line shows the SMM/ACRIM I total irradiance, the dashed line shows the 1'S1 model of sunspots. The corresponding solar images, taken at the San Fernando Observatory, California State University at Northridge, are presented on the upper panel (the plot was provided by courtesy of G. A. Chapman).

State University at Northridge, are presented in the upper panel. As can be seen, when the active regions move onto and rotate out of the solar disk, the effect of bright faculae causes small enhancements in total irradiance. The effect of sunspots is becoming dominant when the active region moves across the center of the solar disk. The dashed line on the lower panel shows the "Photometric Sunspot Index" (PSI), which represents a simple model of the effect of sunspots on total irradiance [23]. PSI relates the area, position and contrast of sunspots to a net effect on the radiative output of the observed solar hemisphere and it is corrected for the limb darkening.

Figs. 3a,b show the relationship between the PSI model and total solar irradiance for the time interval of 1980 to 1994. Note that the original PSI model assumed that the contrast of sunspots was constant [23]. In contrast, results of sunspot photometry show that the contrast of sunspots depends on their area [24] and it changes as a function of the solar cycle [25]. The PSI model shown in Fig. 3b takes into account the area dependence of the contrast of sunspots [26]. As can be seen, dips in total irradiance always correspond to the peaks in the PSI model, convincing the skeptics that the darkening effects of sunspots on total irradiance have indeed been detected and the strong magnetic fields of sunspots can cause negative excursions in the total flux. However, it is a rather surprising observational evidence that in spite of the irradiance deficit due to sunspots, which are the most pronounced at solar maximum, total solar irradiance varies in phase with the solar cycle [6,7]. This indicates that while the strong magnetic fields can reduce the energy transportation within the convective zone, the weak magnetic fields are capable of carrying sufficient amount of extra energy to the solar surface to enhance total irradiance at the time of solar maximum.

The total irradiance corrected for sunspot darkening (hereafter S_c) is shown in Fig. 3c indicating that the solar cycle variability of total irradiance would be considerably larger without the effect of sunspots. Fig. 3d shows the combined Nimbus-7 and NOAA9 Mg II h & k core-to-wing ratio (Mg c/w) [27]. The Mg c/w ratio is calculated from the UV irradiance in the core of the Mg 280 nm line to the irradiance at neighboring continuum wavelengths and

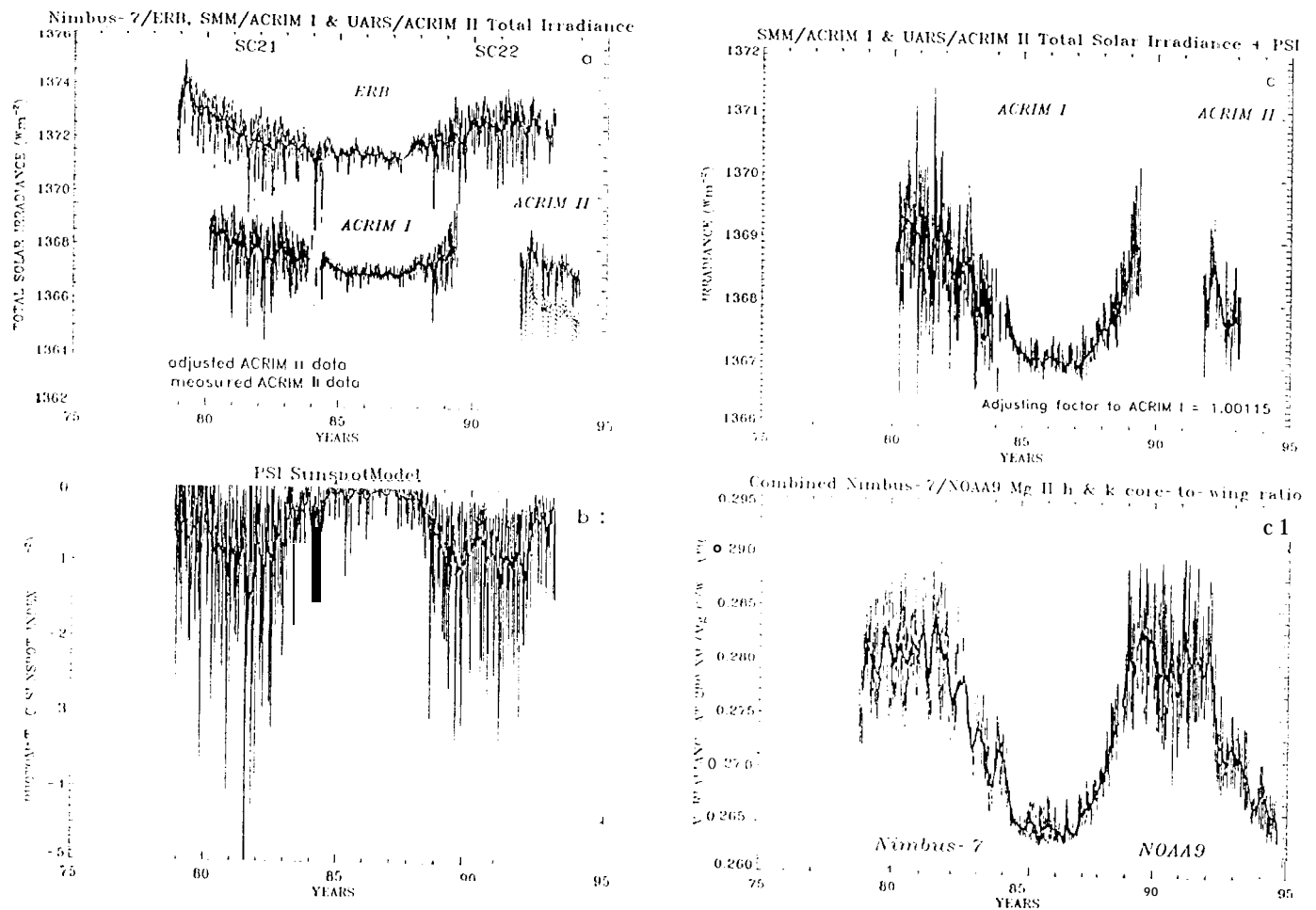


Fig. 3.: The Nimbus-7/ERB and SMM/ACRIM I and UARS/ACRIM II data are presented in Fig. 3a, where the observed ACRIM II data (dashed line) were adjusted to the SMM/ACRIM I scale by [16]. The adjusted data are shown with the solid line. Fig. 3b shows the PSI model of sunspots, Fig. 3c. gives the time series of the ACRIM irradiances after correcting them for the sunspot darkening. The combined Nimbus-7/SBUV1 and NOAA9/SBUV2 Mg II h & k core-to-wing ratio is presented in Fig. 3d.

it has been proven as a good indicator of solar UV variability [28]. Since the formation of the Mg II line is very similar to that of the Ca II K line, it is a reasonably good proxy to describe the effect of the bright magnetic elements. As can be seen from Fig. 3, S_c and the Mg c/w ratio vary in parallel over the solar cycle, indicating that the changing emission of the bright features is the main contributor to the long-term UV and total irradiance variations.

Since the Sun's irradiance is observed from one direction in space, it is difficult to determine whether the observed irradiance variations represent true luminosity changes which occur in the Sun's radiation in all directions or they are simply result of a change in the angular dependence of the radiation field emerging from the photosphere. It has been demonstrated [20,29] that by integrating the solar limb brightness measurements, one can compute the solar luminosity. Using these limb brightness observations, it has been shown that the TIRB and ACRIM total irradiance and the computed luminosity change in phase and relative amplitude [20]. These results demonstrate that the long-term changes are really luminosity changes, which may play an important role in global changes of the Earth's climate. An additional important question is whether the short-term changes in total irradiance are real luminosity changes or they represent a simple re-distribution of the solar radiation by sunspots and active regions faculae [8].

Several theories for explaining the re-radiation mechanism of the missing energy in the sunspot-related irradiance dips have been put forward. Recent numerical convection models of energy and material flowing around a sunspot do not indicate long-term storage of the heat flux, but show that most of the heat flux blocked by sunspot-like objects - magnetic perturbations reappear at the surface; although some of the blocked flux is carried horizontally far from the object [30,31]. In contrast, the "thermal diffusion theory" suggests that the reduced radiation results in storage of the blocked heat flux as thermal and potential energy of the convective zone around a spot, and this energy is re-radiated over the long radiative relaxation time of the layers affected by the spots [32,33,34].

Another explanation suggests that the energy blocked by sunspots is stored in the magnetic fields of the spots [35], in which case sunspots should cause dips in total irradiance during

the early stage of their development, as shown by some of the statistical analyses [36,37]. Formation of sunspots results from the buoyant motion of flux tubes from the solar interior, where the magnetic fields are generated. Since considerable energy is associated with this motion, it is expected that the flux eruption perturbs the luminosity [38,39]. It has been suggested that a slow downward flow is also supposed to occur around the spots during their growing phase that is capable of transporting the blocked energy to surrounding regions where it emerges as facular enhancement [40]. Results of active regions photometry indicates that the facular excess flux compensates the spot deficit on active regions time scale, over several months [22,41]. These controversies indicate that one cannot rule out the possibility that the short-term changes represent real luminosity changes.

3 Modeling Total Solar Irradiance Variations

The detection of total irradiance variations by space-borne experiments during the last two decades stimulated modeling efforts to help identify their causes and to provide irradiance estimates when no satellite observations exist. Although considerable information exists about the variations in total irradiance, the underlying physical mechanisms are not well-understood as yet. Because of the lack of adequate quantitative physical models, one has to rely on empirical models based on “proxy indicators” of solar activity. However, the fundamental question is whether these empirical models can reasonably predict solar irradiance, especially with the long-term precision required by climate studies.

3.1 Modeling Variations on Active Regions Time Scale

The first models - the “Sunspot Blocking Function” and “Photometric Sunspot Index” were developed to explain the effect of sunspots on total solar irradiance [23,32,42]. However, the sunspot models can account for only about half of the variance in total irradiance [22]. The obvious next step was to incorporate the effect of faculae into the models, which were the

potential contributors of the excess flux of total irradiance [23,43]. Results of photometry of active regions indicated that the excess flux of faculae within an active region could not compensate the corresponding irradiance deficit caused by sunspots [22]. In addition, it was found that in numerous cases the effect of sunspots was still clearly resolved after the 1°SI model was subtracted from the observed irradiance values [44]. This residual variability was attributed to the changing ratio of the area of sunspots and faculae during the evolution of active regions [45]. It was also found that in addition to the age of active regions, the rate of growth in the area of sunspots and their magnetic structure played an important role in the short-term variations of total solar irradiance [46,47].

To seek more insight into the role of the evolution of sunspots in irradiance changes, the so-called “active” and “passive” sunspots were separated [46,47]. The “active sunspots” were identified as newly formed and quickly developing sunspot groups. These sunspot groups always had complex magnetic structure (γ and/or δ configuration), when the magnetic polarities were mixed within a group and/or umbra of opposite polarities appeared within the same penumbrae. In addition, these sunspot groups were found to be associated with the largest solar flares and were also identified as Dkc , Bkc , and Fkc types of sunspots in the McIntosh classification system [48]. The “passive sunspots” were defined as old sunspot groups with simple structure and normal (α or β) magnetic polarity conditions. As an example, the time series of the ACRIM 1 total irradiance and the projected area of the active and passive spots are presented for 1980 (solar maximum) and 1984-85 (solar minimum) in Fig. 4. To describe the effect of faculae on total irradiance, the full disk equivalent width of the Hc-line at 1083 nm [49] is also plotted in Fig. 4 [36]. As can be seen, the dips in total solar irradiance are always associated with the peaks in the area of active sunspots. In contrast, the passive sunspots seem to be associated with the temporary enhancements of total irradiance and the peaks in the Hc-line equivalent width.

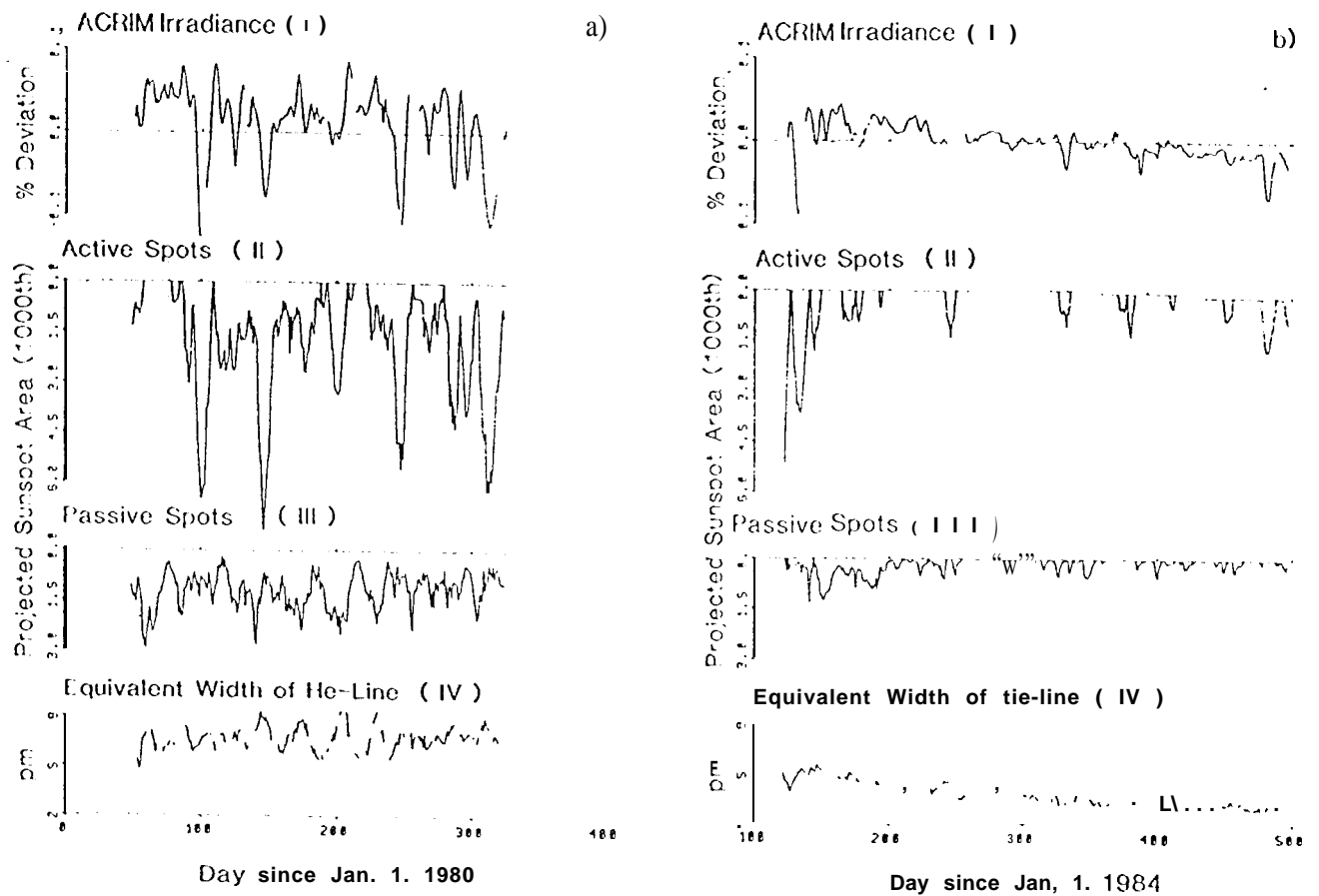


Fig. 4.: The left-side panel gives the time series of the SMM/ACRIM 1 irradiance values (I), projected areas of active sunspots (II), passive sunspots (III) and the full disk equivalent width of the 1 \AA -line at 1083 (IV) for the time interval of February to December of 1980 (maximum of solar cycle 21). The right-side panel shows the same for 1984 and 1985 (minimum of solar cycle '21) (after [36]).

3.1.1. Results of Multivariate Spectral Analysis

The combined effect of sunspots and bright magnetic regions on total solar irradiance has been studied with multivariate spectral analysis [36]. The most important results of multivariate analysis are shown in Fig. 5. The upper panels represent the ACRIM 1 power spectra for the maximum (1980) and minimum (1984-1985) of solar cycle 21. The shaded areas indicate the portion of the ACRIM 1 variance explained by the active spots, passive spots, and the bright magnetic features represented by the H α -line at 1083 nm as a function of frequency. The lower panels give the total squared coherences, which give the portion of total irradiance explained by the combined effect of sunspots and faculae. As can be seen, the squared coherences change as a function of frequency, indicating the changing pattern of the linear association [36].

As can be seen from Fig. 5, more than 90% of the total variance of the ACRIM 1 total irradiance is explained by the combined effect of sunspots and faculae for 1980, whereas only about 73% of the total ACRIM 1 variance is related to sunspots and faculae for solar minimum, when most of the rotational variability of total irradiance (about 80%) is related to the bright magnetic features. In contrast, during solar maximum, the short-term changes in total irradiance are controlled by sunspots; whereas faculae contribute to only about 10% [36]. The lowest curves in the power spectra of the ACRIM 1 total irradiance represent the variations which remain unexplained after removing the effect of sunspots and bright magnetic elements. As can be seen, considerable variation remains unexplained at periods of 51, 27, 13.5, and 9 days, and the amplitude of this residual variation is changing as a function of the solar cycle. However, it is not clear whether this residual variability is related to the uncertainties in the data and/or to additional solar effects which are not yet taken into account in the irradiance models.

3.1.2. Results of Singular Spectrum Analysis

The above exercise demonstrates that before designing a model, the appropriate questions to ask: (1) what are the noise characteristics of the data and (2) how many variables are required

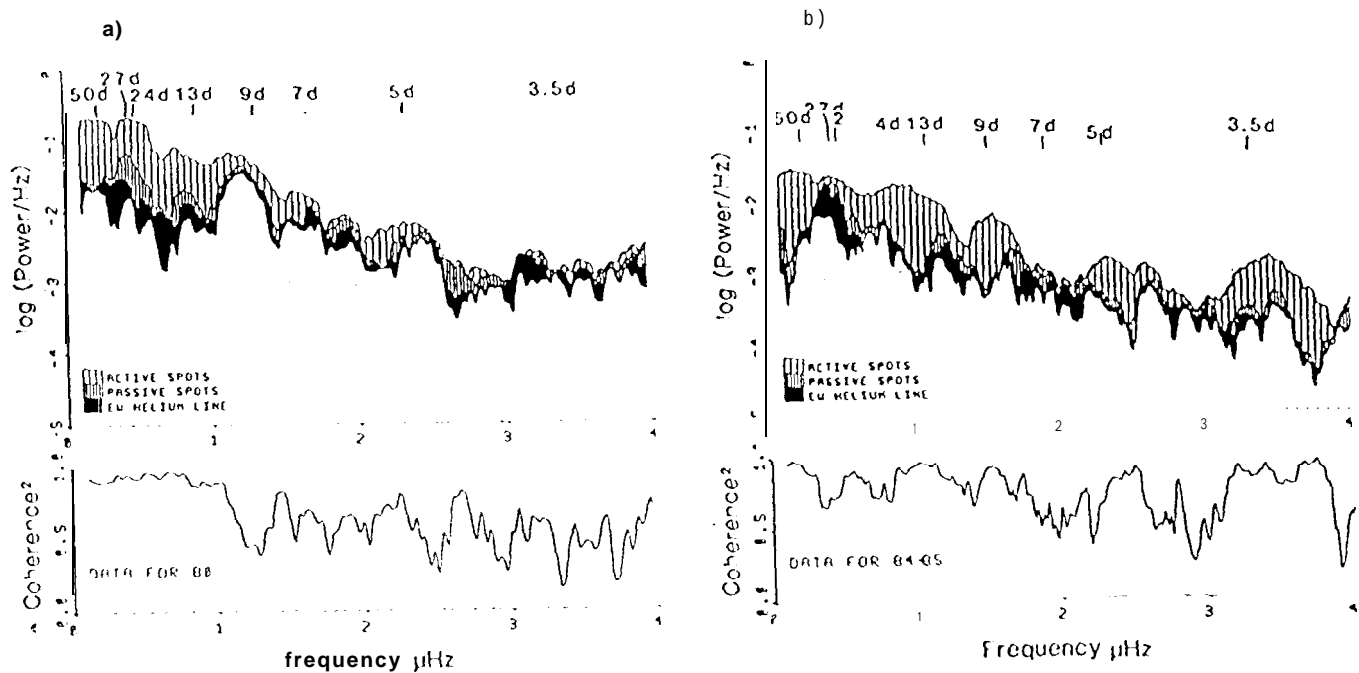


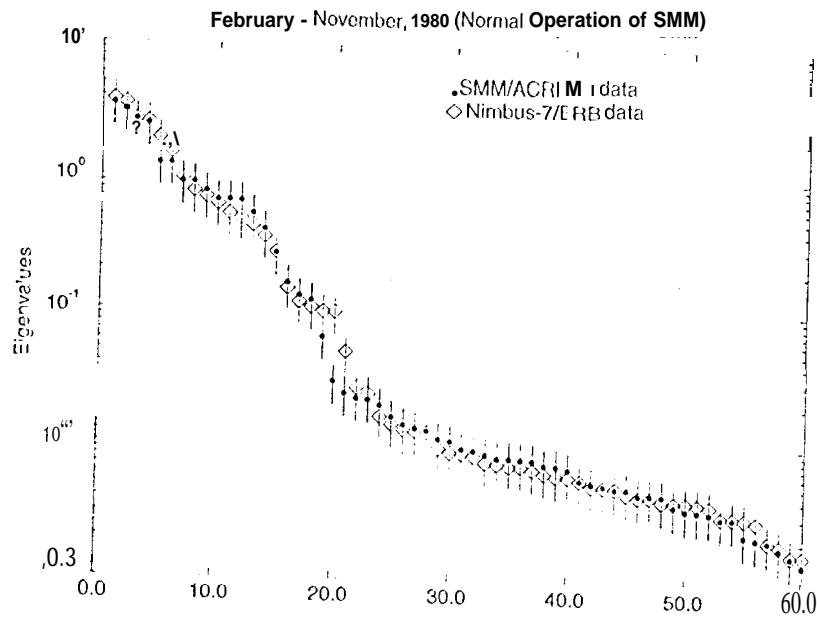
Fig. 5.: The upper panels show the power spectra of the SMM/ACRIM 1 total irradiance for 1980 (left-side) panel and for 1984 - 1985 (right-side) panel (after [36]). The shaded areas indicate the part of the irradiance power explained by the power of the active and passive spots and by the He-line equivalent width at 1083 nm. The total coherence squared values are given in the lower panel.

to reconstruct the observed changes up to the measurement accuracy. An advanced statistical method, “*Singular Spectrum Analysis*” (SSA) has been developed to study and understand nonlinear and chaotic dynamical systems [50] and it has been proven as a powerful method to study irradiance changes [37]. SSA is based on Principal Component Analysis in the time domain. The examined time series is augmented into a number of shifted time series up to a fixed value M . The cornerstone of SSA is the spectral, i.e., eigenvalue-eigenvector, decomposition of the $M \times M$ lagged covariance matrix which is composed of the covariances determined between the shifted time series. The eigenvalues of the lagged covariance matrix compose the so-called Singular Spectrum, where the eigenvalues are arranged in a monotonically decreasing order. The eigenvalues cut-off at a certain order, forming a “tail” in the spectrum which is considered as the noise floor of the data. The number of eigenvalues above the noise floor represents the degree of freedom of the variability, or in other words, the statistical dimension of the data, which is associated with the number of oscillatory components in the signal. The highest eigenvalues represent the fundamental oscillations in the data and in many cases they are related to the trend in the time series.

Results on SSA are illustrated in Fig. 6. Fig. 6a shows the Singular Spectra of the SMM/ACRIM 1 (dots) and the Nimbus-7/ERB (diamonds) radiometers for 1980. The Singular Spectra of the ACRIM 1 and ERB irradiances are very similar and as many as 20 degrees of freedom are established above the noise level of the two sets of total irradiance measurements. The scatter plot diagram between the SMM/ACRIM 1 and Nimbus-7/ERB irradiance is presented in Fig. 6b, which indicates the high correlation ($r = 0.96$) between the two datasets. This confirms that the ERB instrument’s accuracy was much better than the originally estimated $\pm 0.50\%$ [12] and for the time interval of 1980 the two different radiometers resolved the same oscillations in total irradiance. Note that in 1980, during the normal operational mode of the SMM satellite, the measuring precision of ACRIM 1 was so high ($\pm 0.002\%$) that each observed event had a solar, rather than instrumental, origin [51].

Unfortunately, in December 1980 the solar pointing system of the SMM satellite failed and it

Singular Spectra of the ACRIM I and ERB Data



Comparison of the ACRIM I and ERB Data

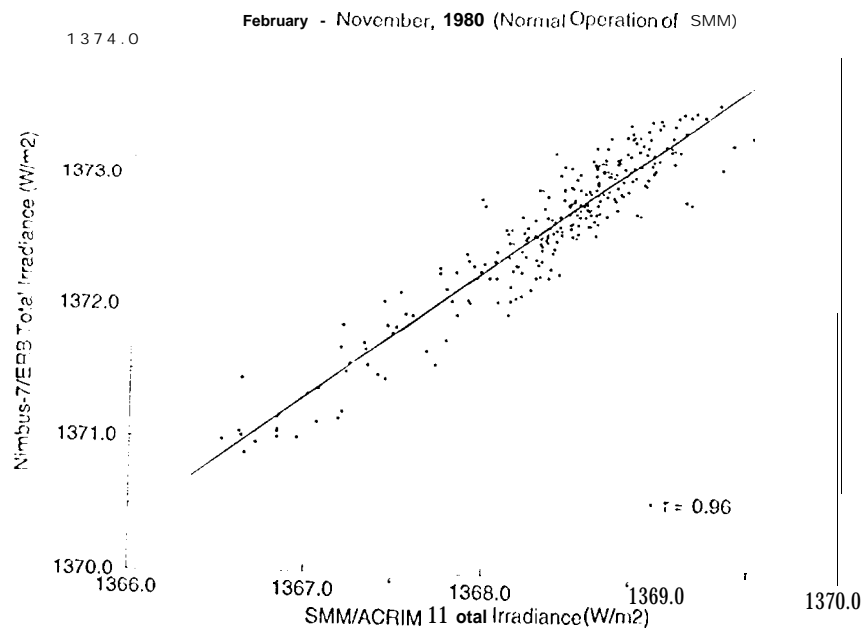


Fig. 6.: The Singular Spectrum of the SMM/ACRIM I total irradiance for the time interval of February to November, 1980 (normal operational mode of the SMM satellite) is presented in Fig. 6a by the dots. The diamonds give the Singular Spectrum of the Nimbus-7/ERB data for the same time interval. The scatter plot diagram between the ACRIM I and ERB data is given in Fig. 6b.

Singular Spectra of the ACRIM I and ERB Data

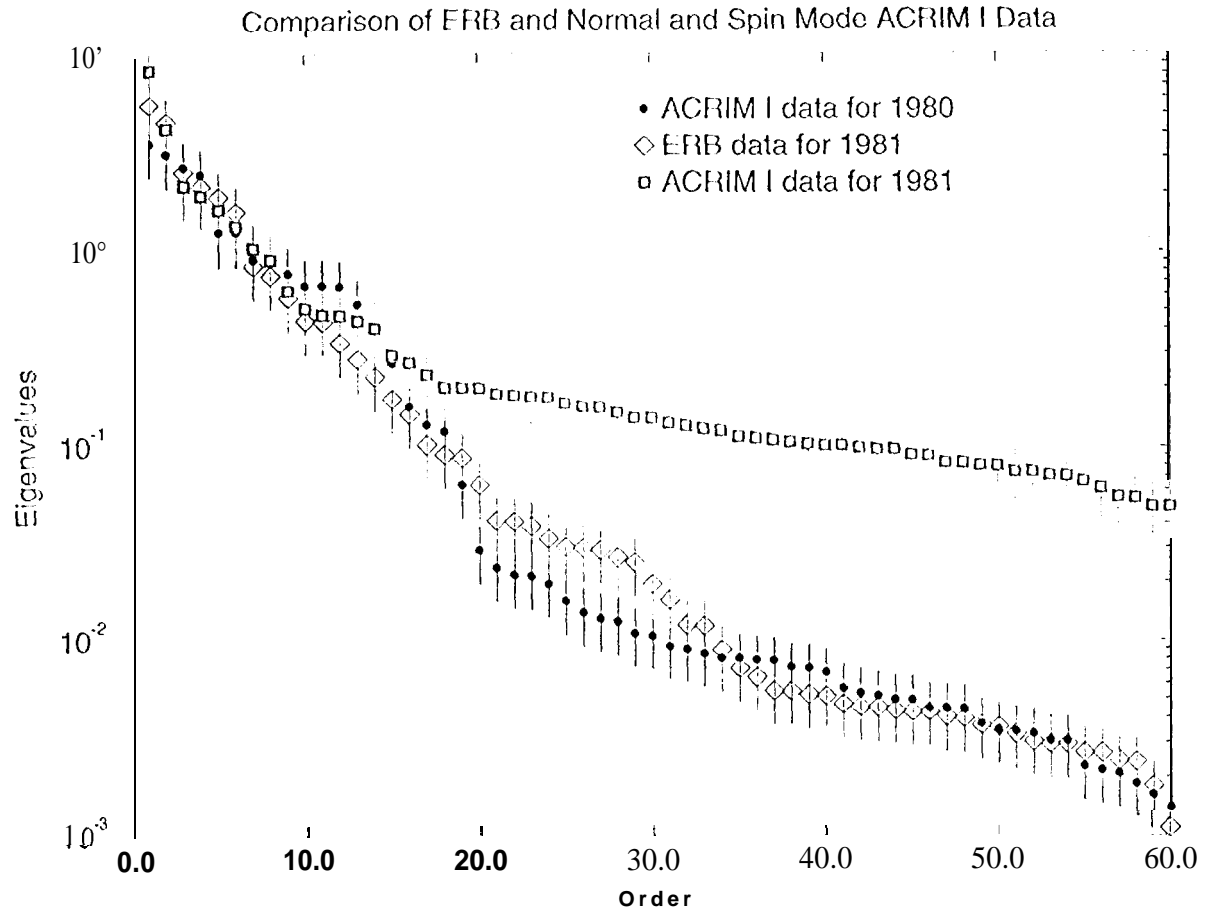


Fig. 7.: The Singular Spectra of the Nimbus-7/ERB data as well as the normal and spin operational mode of ACRIM I data are presented. The dots give the ACRIM I data for 1980 (normal operational mode of SMM). The diamonds show the Nimbus-7 data for 1981, the squares give the ACRIM I data for the spin operational mode in 1981.

was placed into the so-called “spin operational mode” until April 1984 when the solar pointing system of the satellite was repaired by a space shuttle mission. During the spin operational mode the measuring precision of ACRIM 1 decreased by about a factor of 5 (from 0.002% to 0.01 %) [51]. The Singular Spectrum of the Nimbus-7/ERB data (diamonds) is presented in Fig. 7 for 1981, the squares in Fig. 7 give the Singular Spectrum of the spin-mode ACRIM 1 data in 1981. To compare the normal and spin operational mode of ACRIM 1 data, the plots show the eigenvalues of ACRIM 1 for 1980. As shown in Fig. 7, no significant change can be recognized between the Singular Spectra of the ACRIM 1 data for 1980 and the ERB data for 1981. In contrast, the Singular Spectrum of the spin mode ACRIM 1 data is quite different, i.e., the noise level increased significantly and only a few oscillatory components can be resolved from these data. Note that the correlation coefficient between the ERB and ACRIM 1 data for 1981 is also reduced to $r = 0.80$. The results presented in Fig. 7 demonstrate that the change in the ACRIM 1 Singular Spectra from 1980 to 1981 is not related to the changing level of solar activity as the solar cycle progressed, but it has been related to the reduced measuring accuracy and precision of the ACRIM 1 instrument during the spin operation mode of SMM because of the lack of proper solar pointing and the lack of normal duty cycle of ACRIM 1 [52]. Unfortunately, the reduced accuracy and precision of the spin mode data impose a serious constraint on the long-term precision of the entire ACRIM 1 database which makes it difficult to study the change in the various oscillatory components of the ACRIM 1 total irradiance as a function of solar cycle [53].

The most interesting aspect of SSA is the reconstruction of the examined time series above the noise level and/or part of interest. The various oscillatory components in the examined time series can be reconstructed as a projection to the so-called “Empirical Orthogonal Functions”, which are the eigenvectors of the covariance matrix [50]. The main oscillatory components between periods of 10 to 51 days have been reconstructed for the normal operation mode of ACRIM 1 data in 1980 (Fig. 8) and for the projected areas of active (Fig. 9) and passive sunspots (Fig. 10), respectively. As can be seen from Fig. 9, the first four eigenvalues in total

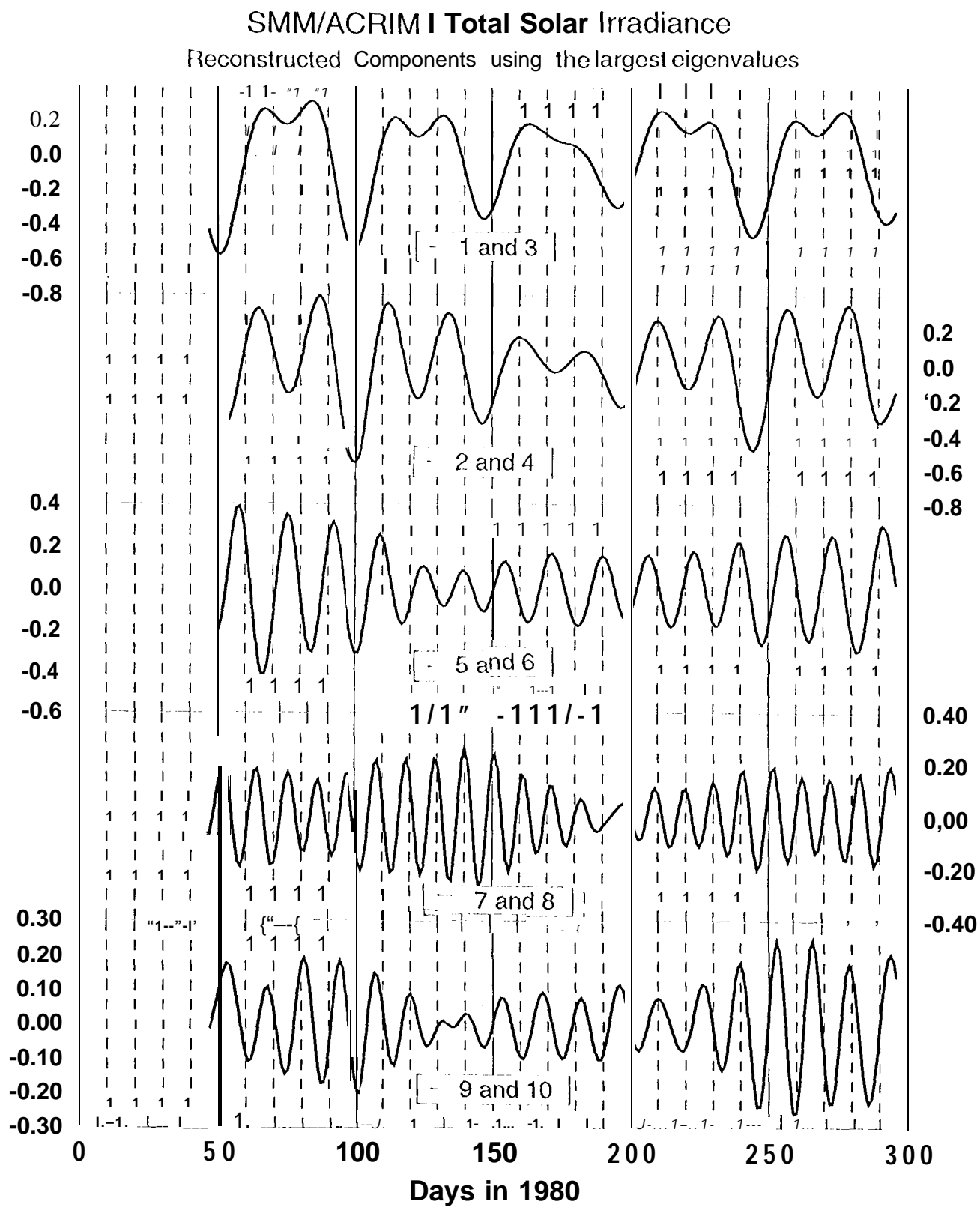


Fig. 8.: The first ten Reconstructed Components of the SMM/ACRIM I data are presented for 1980.

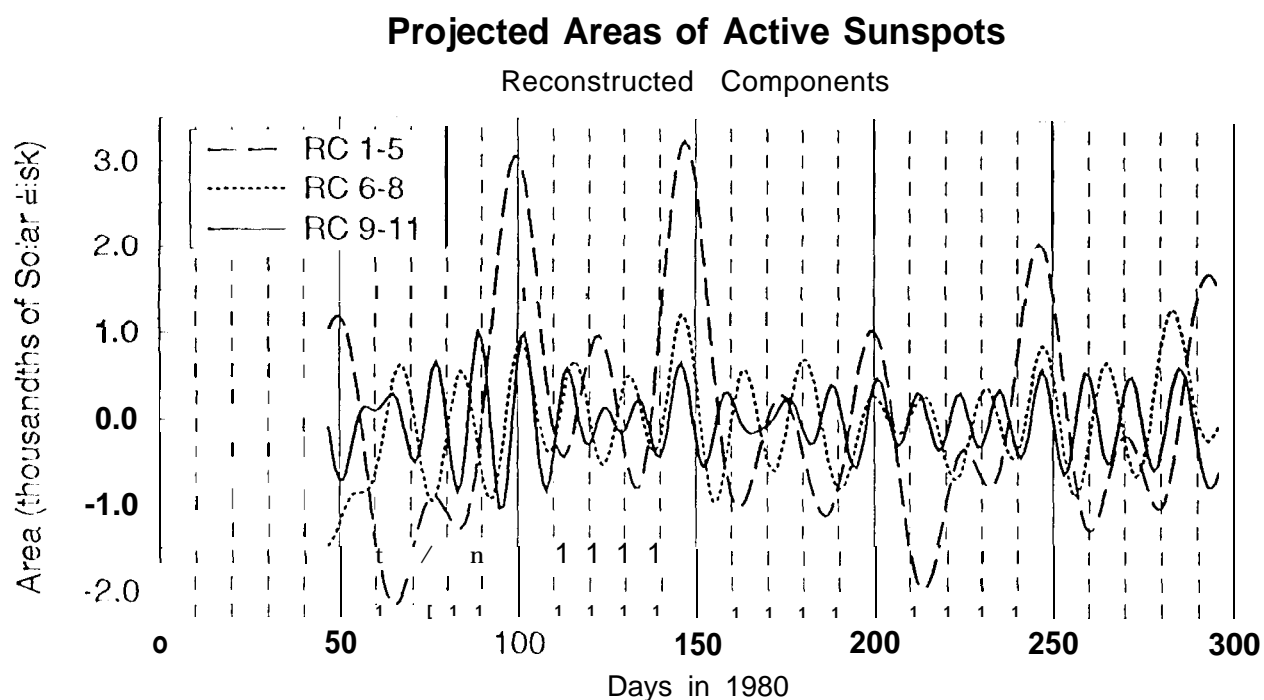


Fig. 9.: The Reconstructed Components of the projected areas of active sunspots groups are presented for 1980.

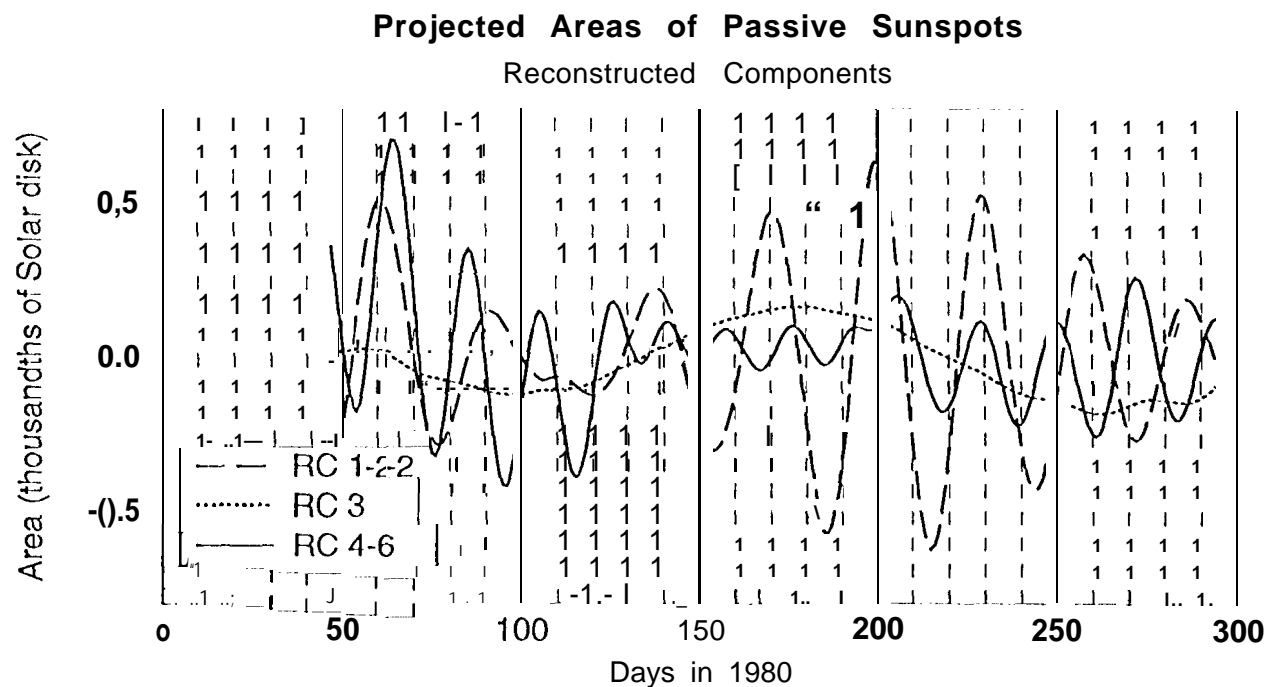


Fig. 10.: The Reconstructed Components of the projected areas of the passive sunspot groups are presented for 1980.

irradiance represent the 50 and 25 days oscillations [36,45,46]. The first five eigenvalues in the projected areas of active sunspots represent the peaks at 50 and 25 days, which correspond to the dips in the first four RCs of total irradiance. Since the oscillations at 50 and 25 days always occur together, it is a strong indication that these periods are harmonics of each other. These two dominant oscillations are completely missing from the projected areas of passive spots. In that case the largest eigenvalue represents a 30-day variation, which is the most pronounced in the second part of 1980, when many old regions occurred on the Sun [37].

3.2 Modeling Variations Over the Solar Cycle

Construction of long-term models of total irradiance has been of high interest because they may help to understand the role of irradiance variations in climate changes [10]. In the discussion to follow we will address the question of the accuracy and limitation of the current empirical models of total irradiance. These are extremely important issues which need attention, especially when irradiance models are extrapolated back to the time of the Maunder Minimum.

A particular model of total irradiance is presented in Fig. 11. The dotted lines show the 81-day running means of the modeled irradiance values calculated with multiple linear regression based on the formula: $y = a + bX + cX^2$, where a , b , and c are the regression coefficients. X represents the $1/S1$ function, whereas X^2 is the $Mg\ c/w$. y gives the best-fit linear relationship between total irradiance and sunspots as well as the bright magnetic elements represented by the $Mg\ c/w$ ratio. The model has been calculated for the time interval of the SMM/ACRIM 1 measurements of 1980 to 1989 and it was extended to the end of 1993, in a similar fashion as described in [54] in order to compare the observed and predicted irradiance values.

The heavy line in Fig. 11a shows the 81-day running means of the SMM/ACRIM 1 and UARS/ACRIM 11 total irradiance. Note that in this case the ACRIM 11 data were scaled to the ACRIM 1 level via the intercomparison of the two ACRIM datasets with the ERB and ERBS irradiance measurements (adjusting factor = 1.00115) [16]. In Fig. 11b, the adjusting factor (1.001802) was calculated from the ERB/ACRIM 1 and ERB/ACRIM 11 ratios [14], yielding

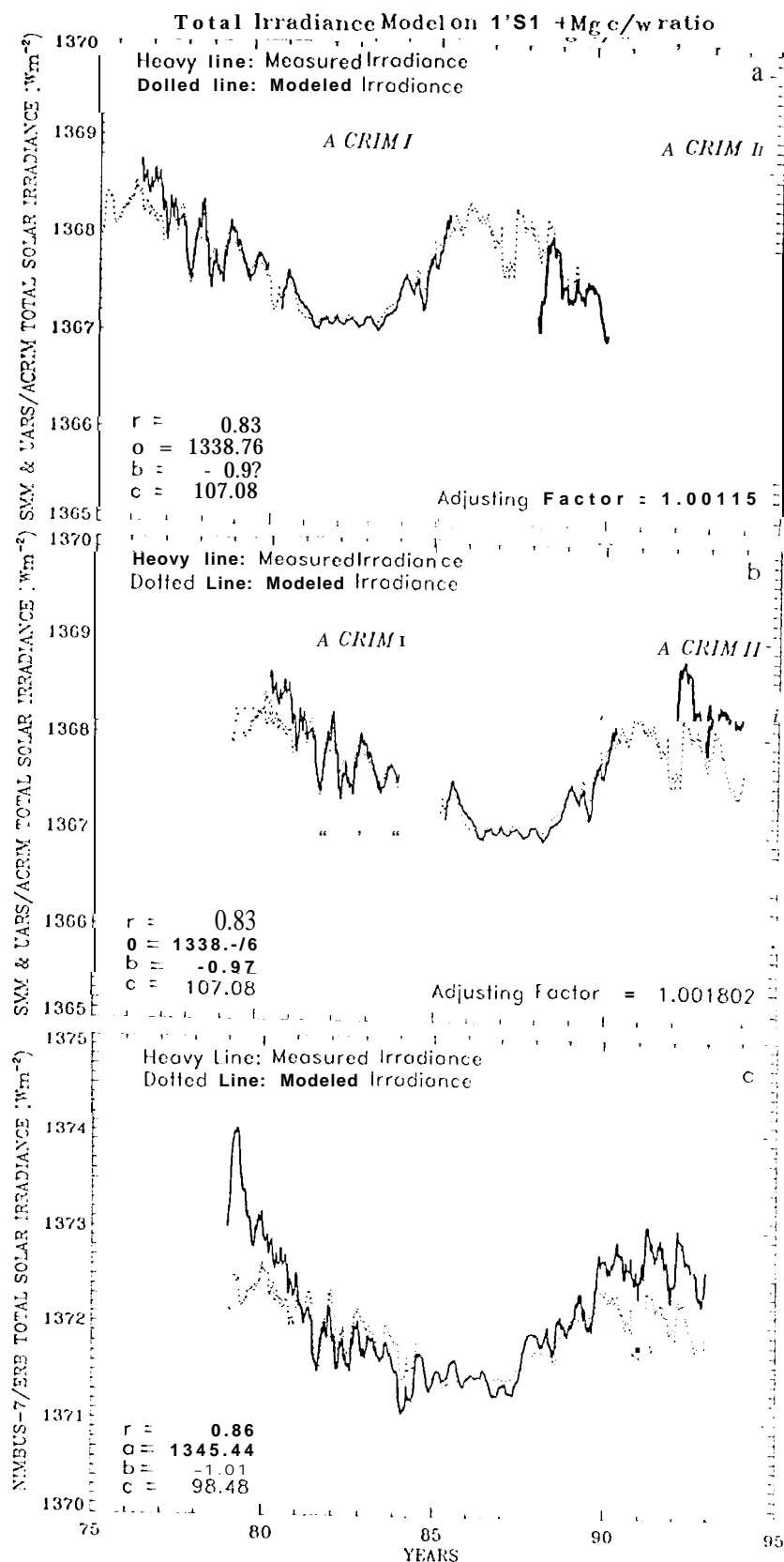


Fig. 11.: The heavy lines show the 81-day running means of the observed total solar irradiance, the dotted lines present the 81-day running means of the multiple regression models. In Fig. 11a the ACRIM II data are adjusted to the ACRIM I level via the intercomparison of the two ACRIM datasets with the ERB and ERBS data [16], in Fig. 11b the scaling is performed on the basis of the ERB and ACRIM intercomparison [14]. The heavy line in Fig. 11c shows the Nimbus-7/ERB total irradiance.

to higher ACRIM 11 values than presented in Fig. 11a. The heavy line of Fig. 11c shows the 81-day running means of the Nimbus-7/TIRB data. As can be seen from Fig. 11, there is a reasonably good agreement between the observed and estimated irradiance values for the declining portion of solar cycle 21 and the rising portion of solar cycle 22 as well as for solar minimum. However, the regression models presented in Fig. 11 underestimate the observed irradiance changes at the maximum of solar cycle 21, similar to models based on the Ca II K index, He I line at 1083 nm and the 10.7 cm radio flux [7,21,54,55]. At the maximum of solar cycle 22, the predicted irradiance values also underestimate the Nimbus-7/TIRB irradiance as well as the ACRIM 11 values when they are scaled to the ACRIM 1 level by means of the higher adjusting factor [14]. In contrast, using the lower adjusting factor (1.00115) [16], the “predicted” and “measured” irradiance values match each other quite well.

It has been a long-debated (and still unresolved) issue whether the unexplained variability at solar maximum is related to instrumental effects [21], uncertainty of the data and limitation of the modeling techniques [54,56,57], and/or it represents real variability related to additional solar effects, such as surface temperature changes [20,29], radius changes [58], and/or large scale motions [59].

3.2.1. Uncertainties of Irradiance Measurements

It has been suggested that the discrepancy between the observed and estimated irradiance in 1 W0 was simply related to the degradation of the ACRIM 1 radiometer at the beginning of its operation [21]. However, the difference between the ACRIM 1 total irradiance and its regression models was about 300 ppm for 1980, which is almost one third of the peak-to-peak irradiance change observed during solar cycle 21 [13]. The degradation of the ACRIM 1 radiometer over its 9.5 years operation was 600 ppm, which was corrected to a 50 ppm level through the so-called “phase operational mode” of the three cavities of the ACRIM 1 instrument [13]. Note that the degradation of the radiometers is primarily caused by their exposure to high energetic solar fluxes, such as EUV, UV, and particle fluxes. To control the

degradation, the ACRIM instruments consist of three cavities. The so-called “primary cavity” observes the Sun continuously, whereas the two other cavities are exposed to the solar radiation only from time to time. Intercomparison of the measured irradiance values by the primary and “back-up” cavities makes it possible to minimize the degradation of the instrument [4, 3, 14, 51]. Therefore, the observed 300 ppm difference between the measured and modeled ACRIM 1 data during 1980 is well-above the “calibrated” degradation of the ACRIM 1 instrument. In addition, the Nimbus-7/ERB radiometer, during the second year of its operation, showed the same trend as the ACRIM 1 instrument for 1980, indicating that the discrepancy between the estimated and measured total irradiance is a real, rather than instrumental, effect.

Unfortunately, we do not have adequate knowledge about the variations in total solar irradiance at the maximum time of solar cycle 22. The observations of the SMM/ACRIM 1 radiometer ended its operation just before the maximum of solar cycle 22 and the ACRIM II observations started almost two years after the demise of the SMM satellite [14]. As illustrated in Fig. 11, it is not obvious how to scale the ACRIM 1 and ACRIM II data to the same level and what is the accuracy of this procedure. It has been shown that an 0.4 W/m^2 upward drift occurred in the Nimbus-7/ERB data in the time frame of September and October, 1989, which was followed by another drift with a similar amplitude between 1990 and 1993 [60, 61]. The Nimbus-7/ERB data have not yet been corrected for these drifts, which may explain the difference between the two adjusting factors [14, 16] and the different levels of the ACRIM 1 I data presented in Figs. 11 a and 11 b, respectively. It must be underscored, on the other hand, that (1) the *large uncertainty* of the ACRIM 1 data during the *spin operational mode* of SMM [55], (2) the obvious *discrepancy* between the ACRIM 1 and ERB data *during solar minimum* [16], and (3) the “*inverse degradation*” of the ACRIM II instrument [14] further complicate the calculation of the correct scaling factor between the ACRIM I and ACRIM II measurements. Finally, the ERBS instrument performs observations only on a biweekly basis [15, 60], therefore the ERBS total irradiance variability may be highly affected by the effect of sunspots, especially during solar maximum. This may introduce additional uncertainties into the adjustment of the

UARS/ACRIM 11 data to the SMM/ACRIM 1 level.

3. 2. 2. Limitation of the Irradiance Models

Besides the instrumental problems and the described uncertainties in the data, we must also consider that the empirical models fail at solar maximum because of a change in how the solar atmosphere responds to the presence of strong magnetic fields sustained over the 2-3 years of solar maximum. The empirical regression models derived from full disk surrogates of total irradiance provide only a general information on the observed irradiance variations and they are controlled by the ascending and descending phases of the solar cycle and not by the mutual behaviour of the various measurements during solar maximum [56]. In addition, the time series of solar irradiances either space-borne or ground-based surrogates can be regarded as “pseudo-periodic” signals with variable spectral properties (e.g. change of periods, amplitudes, and phases) [36,61]. Therefore, it may be that we do not have the same empirical transformations between total irradiance and its surrogates, such as the Ca II K, 10.7 cm radio flux, H α line at 656 nm, and the Mg c/w ratio at solar maximum as during the periods when the emerging magnetic flux is both low and changing steadily at the beginning and the end of the solar cycle [56]. As shown by the results of SSA (Figs. 6,7), there are many oscillatory components in total solar irradiance, whereas the current empirical models are based only on three components: the quiet Sun, active regions and the magnetic network components.

In addition to the simplicity of the currently used modeling techniques, one of the largest obstacles of proper irradiance modeling is the lack of long-term adequate spatially resolved data. The irradiance monitoring experiments observe the Sun as a star, therefore they cannot reveal the underlying physical mechanisms. To identify the causes of the observed irradiance changes, one needs to study high resolution and high precision solar images. The largest constraints in irradiance modeling is the poor record of the photospheric faculae. Because of this, the effect of faculae is modeled by chromospheric surrogates, such as the Ca II K plages, Mg c/w ratio, H α line at 656 nm, 10.7 cm radio flux, although more than 90% of the total solar flux is

emitted from the photosphere. However, the conversion factor between the **area** and intensity of photospheric faculae and chromospheric plages is not known, the center-to-limb behaviour of the contrast of white light faculae is quite different than that of the plages [62]. The variability of the 11 μ m line and the 10.7 cm radio flux is rather complex and both indices have coronal contributions which are not present in total irradiance [63]. About 15% of the variations in the 11 μ m line is related to dark filaments [64], and the effect of filaments is also present in the Ca II H and Mg II lines. A considerable variation of the 10.7 cm radio flux is related to the strong magnetic fields of sunspots, especially during high solar activity conditions, whereas another part is due to the effect of weaker fields of plages [63]. In addition to the complexity of the variations of these indices, they are full disk indices, therefore they provide no information about the temporal and spatial distribution of various magnetic features causing irradiance changes.

It also must be noted that the term of the active network is too large and not well-defined and its contribution to irradiance changes has not been identified quantitatively. In addition, the quiet-Sun component still must be separated. It is not yet clear whether there is a slow secular change both in the network and/or globally in the Sun [56]. As mentioned before, the sunspot models used in irradiance modeling have also considerable constraints, such as the lack of high precision measurements of the area and position of sunspots; the inaccurate knowledge of the change of the contrast of sunspots as a function of their evolution and the solar cycle.

4 Conclusions

Measurements of the solar energy output and understanding its variability are extremely important since they provide information about the physical processes in, below, and above the solar photosphere. On the other hand, the terrestrial implication of the changes in the solar electromagnetic flux is essential, since the major portion of the solar energy output reaches the troposphere and the Earth's surface and oceans, and its long-term changes may be responsible

for slow climate changes such as produced the Little Ice Ages. Therefore, long-term and high precision measurements of total irradiance are essential to study and understand the climate impact of solar irradiance variability.

Measurements of total irradiance from space over the last two decades convinced the skeptics that the solar energy output is not constant but it varies over a wide range of periodicities, and most of the observed changes are associated with the solar magnetic activity [6,7,8]. Although considerable information exists on solar irradiance variability, the underlying physical processes are not yet understood. Because of the lack of quantitative physical models of total irradiance variability, one has to rely on empirical models developed from surrogates of solar magnetic activity. However, one has to keep in mind that the physics of the formation of the solar radiation integrated over the entire spectrum and the used magnetic surrogates is not identical, the current irradiance models can estimate total irradiance with only a *few percent of accuracy* [57] which is less than sufficient to reconstruct and predict long-term irradiance changes based on the current empirical models of total irradiance, especially back to the time of the Maunder Minimum.

Unfortunately, the current irradiance database does not have either the long-term precision, which is required to study the solar induced climate changes. As described in this paper, there are no accurate measurements of total irradiance at the maximum of solar cycle 22, and no correct procedure has been developed to adjusting the SMM/ACRIM1 and UARS/ACRIM11 time series. Therefore, in spite of the fact that the space-borne irradiance observations cover almost two solar cycles, these measurements do not provide sufficient information to establish the *amplitude of the change in total irradiance between solar maximum and minimum* - the two extrema of the activity cycle which are the most determining factors in the changes of the terrestrial climate.

Finally, it must be emphasized that global effects, such as changes in the differential rotation in the solar interior, a solar dynamo magnetic field near the bottom of the convective zone, and/or large scale convective cells may also produce long-term changes in the solar luminosity

[8]. If that is the case, we will not be able to reproduce the changes in total irradiance from the surface manifestations of solar magnetic activity. Observations of global solar parameters, such as the solar diameter and the frequency changes of solar p-mode oscillations may provide additional tool to study and understand irradiance changes. However, as described throughout this paper, there is more than enough evidence that neither theory nor the empirical models can replace direct irradiance measurements. Therefore, to continue the direct, uninterrupted observations of total irradiance with high precision and accuracy is inevitable in the following decades.

Acknowledgements: The research described in this paper was carried out by the University of California and the Jet Propulsion Laboratory, California Institute of Technology under a contract with the National Aeronautics and Space Administration. The SMM/ACRIM 1 and 11A RS/ACRIM II data used in this study have been produced by the Active Cavity Radiometer Irradiance Monitoring Group at JPL, and have been published in the NOAA/WDC Solar Geophysical Data Catalogue. The Nimbus-7/TRE data were kindly provided by Dr. D. Hoyt. The author expresses her gratitude to the entire SOHO/VIRGO Science team for providing the first VIRGO results for this paper. The author acknowledges the NASA/GSFC ozone processing Team (OPT) for the Nimbus-7 SBUV/1 data and the NOAA/NESDIS for the SBUV/2 data, which were kindly provided by L. Puga. The NSO/Kitt Peak H α -line measurements are produced co-operatively by NSF/NOAO, NASA/GSFC, and NOAA/SEL and were provided by courtesy of Dr. J. Harvey. The useful comments of S. Baliunas, R. Helizon, D. Parker, R. Ulrich, P. Varadi, are highly appreciated.

References

- 1 Fröhlich, C., in *The Solar Output and its Variation*, edited by O.R. White (Colorado Assoc. Univ. Press.) 1977, pp. 93-110.
- 2 Crommelynck, J., *J.R.M. Publication Series A*, **81**(1973), 1-50.

- 3 Hickey, J.R. and Karoli, A., *Applied Optics*, **13** (1974) 523-533.
- 4 Willson, R.C., *Appl. Optics*, (1979)
- 5 Brusa, R.W. and Fröhlich, C., *Appl. Optics*, **25** (1986) 4173.
- 6 Willson, R.C. and Hudson, H. S., *Nature*, **332** (1988) 42.
- 7 Fröhlich, C., in *The Sun as a Variable Star: Solar and Stellar Irradiance Variations*, edited by J.M. Pap, J., C. Fröhlich, C., H. S. Hudson and S.K. Solanki (Cambridge Univ. Press) 1994 pp.28-36.
- 8 Hickey, J., in *Global Changes in the Sun*, edited by J. Roca Cortes, (Cambridge Univ. Press) 1996, in press.
- 9 Nesme-Ribes, E., Sokoloff, D., and Sadourney, R., in *The Sun as a Variable Star: Solar and Stellar Irradiance Variations*, edited by J.M. Pap, J., C. Fröhlich, C., H.S. Hudson and S.K. Solanki (Cambridge Univ. Press) 1994 pp. 244 - 251.
- 10 Jean, J., Beer, J., and Bradley, R., *Geophys. Res. Letters*, **Vol. 22, No. 23** (1995) 3195.
- 11 Fröhlich, C., Andersen, B., Appourchaux, T., Berthomieu, G., Crommelynck, D., Domingo, V., Fichot, A., Finsterle, W., Gómez, M., Gough, D., Jiménez, A., Jefferies, T., Lombaerts, M., Pap, J., Provost, J., Roca Cortés, J., Romero, J., Roth, H., Sekii, T., Telljohann, S., Toutain, T., Wehrli, Ch., *Solar Phys.* (1996), in press.
- 12 Kyle, H.L., Hoyt, D. V., and Hickey, J.L., *Solar Phys.*, **152** (1994) 9.
- 13 Willson, R.C. and Hudson, H. S., *Nature*, **351** (1991) 472.
- 14 Willson, R.C., in *The Sun as a Variable Star: Solar and Stellar Irradiance Variations*, edited by J.M. Pap, C. Fröhlich, H. S. Hudson, and S.K. Solanki (Cambridge Univ. Press.) 1994 pp. 54-62.

- 15 Mecherikunnel, A., *Solar Phys*, **152** (1994) 125.
- 16 Fröhlich, C., in *The Proceedings of the SOLFIRS22 1996 Workshop*, edited by J.M. Pap, C. Fröhlich and R.K. Ulrich (Kluwer Academic Publishers 1996, in press
- 17 Crommelynck, D., Domingo, V., Fichot, A., Fröhlich, C., Penelle, B., Romero, J., and Wehrli, Ch., *Metrologia* 30 (1 993) 375.
- 18 Romero J., Wehrli, Ch., and Fröhlich, C., *Solar Phys.*, **152** (1994) 23.
- 19 Fröhlich, C., C. Romero, J. Roth, Wejrli, C, Andersen, B., Appourchaux, T., Domingo, V., Telljohann, H., Berthomieu, G., Crommelynck, D. Chevalier, D., Fichot, V., Däppen, A., Gough, Hoksena, D.O., Jiménez, A., Gomez, M., Herreros, J., Roca-Cortés, T., Jones, A.R., Pap, J., and Willson, R. C., *Solar Phys.* 162] 996, 101.
- 20 Kuhn, J., Libbrecht, K.G. and Dicke, H.H., *Science*, 242 (1 988) 908.
- 21 Foukal, P. and Lean, J., *Ap. J.* 328 (1988) 347,
- 22 Chapman, G. A., *Ann. Rev. A siren. A strophys.*, 25 (1 987) 633.
- 23 Hudson, H .S., Silva, S., Woodard, M. and Willson, R. C., *Solar Phys.*, **76**(1982) 211!
- 24 Steinegger, M., Brandt, D., Pap, J., and Schmidt, W'., *Astrophysics and Space Science*, 170 (1990) 127.
- 25 Maltby P., Avrett, B.H., Carlsson, M., Kjedseth-Moe, O., Kurucz, J{.1.,, and Loeser R., *Ap. J.*, 306 (1986) 284.
- 26 Fröhlich, C., Pap, J., and Hudson, H. S., *Solar Phys.*, **152 (1994)** 111.
- 27 Donnelly, J{.1.", White, O.R., and Livingston, W.C., *Solar Phys.*, 152 (1994) 69.
- 28 Leath, D.F. and Schlesinger, B.M., *J. Geophys, Res*, 91 (1986) 8672.

- 29 Kuhn, J. and Libbrecht, K. G., *Ap. J. Letters*, **381** (1991) L35.
- 30 Fox, P. A., Sofia, S., and Chan, K. L., *Solar Phys.*, **135** (1991) 15.
- 31 Lydon, T. J., Fox, P., and Sofia, S., *Ap. J.*, **403** (1993) 179.
- 32 Foukal, P., in *Physics of Sunspots*, edited by L. Cram and J. Thomas (SPO Publ.) 1981, pp. 391.
- 33 Spruit, H., *Astron. Astrophys.*, **108** (1982) 360.
- 34 Foukal, P., Fowler, L. A., and Livshits, M., *Ap. J.*, **267** (1981) 863.
- 35 Wilson, P., in *Physics of Sunspots*, edited by L. Cram and J. Thomas (SPO Publ.) 1981, pp. 83-97.
- 36 Fröhlich, C. and Pap, J., *Astron. Astrophys.* **220** (1989) 272.
- 37 Pap, J. and Varadi, F., in *Solar Drivers of Interplanetary and Terrestrial Disturbances*, edited by K. S. Balasubramanian, S. L. Keil, and R. N. Smartt (IAGG) 1996, pp. 576 - 585.
- 38 Chou, 1987
- 39 Hudson, H. S., *Ann. Revs. Astron. Astrophys.*, **26** (1988) 473.
- 40 Schatten, K. S. Mayr, H., Omidvar, K., and Maier, M., *Ap. J.*, **311** (1986) 460.
- 41 Steinegger, H., Vázquez, H., Bonet, J. A., and Brandt, D., *Ap. J.*, **461** (1996) 478.
- 42 Hoyt, D. and Eddy, J., *NCAR/TN-194 + STR*, 1982, NCAR Technical Notes.
- 43 Sofia, S., O'Keefe, J., Lesh, J. J., and Endal, A. S., *Science* **204** (1982) 1306.
- 44 Willson, R. C., Gulkis, S., Janssen, H., Hudson, H. S., and Chapman, G. A., *Science*, **211** (1981) 700.

- 45 Willson, R.C., *J. Geophys. Res.*, **86** (1982) 4319,
- 46 Pap, J., *Solar Physics*, **97** (1985) 21
- 47 Pap, J., *Astrophys. Space Sci.*, **127** (1986) 55.
- 48 McIntosh, P., *Solar Phys.*, **125** (1991) 257.
- 49 Harvey, J., in *Proceedings of Solar Irradiance Variations on Active Regions Time Scales* edited by B. J. LaBonte, G.A. Chapman, H.S. Hudson, and R.C. Willson, (NASA-CRP 2310) (1984) pp. 197-211.
- 50 Vautard, R., Yiou, P., and Ghil, M., *Physica D*, **58** (1992) 95.
- 51 Willson, R.C., *Space Science Reviews*, **38** (1984) 203.
- 52 Fröhlich, C., Foukal, P., Hickey, J.R., 1111(1991), 11.s., and Willson, R.C., in *The Sun in Time* edited by C.D. Sonett, M.S. Giampapa, and M.S. Matthews, (Univ. Arizona Press, Tucson) 1991, pp. 11-29.
- 53 Pap, J. and Varadi, P., in preparation
- 54 Pap, J., Willson, R.C., Fröhlich, C., Donnelly, R.F. and Puga, L., *Solar Phys.*, **152** (1994) 13.
- 55 Brandt, P., Stix, M., and Weinhardt, W., *Solar Phys.*, **152** (1994) 119.
- 56 Pap, J., Vigouroux, A. and Delache, Ph., *Solar Phys.*, **167** (1996) 125.
- 57 Pap, J. and White, O.R., in *The Solar Engine and its Influence on Terrestrial Atmosphere and Climate*, edited by E. Nesme-Ribes *NATO ASI Series, Springer - Verlag, Berlin*, 1994 pp. 235.
- 58 Ulrich, R. and Bertello, E., *Nature*, **377** (1995) 214.

- 59 Ribes, E., Mein, P., and Mangeney, A., *Nature*, **318** (1985) 170.
- 60 Lee, M. H., Gibson, M. A., Wilson, R. S., and Thomas, S., *J. Geophys. Res.*, 100 (1995) 1667.
- 61 Chapman, G. A., Cookson, A. M., and Dobias, J. J., *J. Geophys. Res.* 101, (1996) [3,54].
- 62 Bouwer, D., *Solar Phys.*, **142** (1992) 365.
- 63 Tapping, P., *J. Geophys. Res.*, 92 (1987) 829.
- 64 Harvey, J.W. and Livingston, W.C., in *Solar Infrared Astronomy*, edited by D. Rabin, J. Jeffreys, and C. Linsey (Kluwer Academic Publishers) 1994, pp. 59 - 64